

Numerical approach to estimate the accuracy of ultrasonic flowmeter under disturbed flow condition

He-ming Hu, Chi Wang, Tao Meng

Division of Thermometry and Materials Evaluation, National Institute of Metrology, China
No.18, Bei San Huan Dong Lu, Chaoyang Dist, Beijing, P. R. China
Phone: +86-010-6452-5122, E-mail: huhm@nim.ac.cn

Abstract: The multi-path ultrasonic flowmeter is a well established method for accurate discharge measurement in large closed conduits. Although multi-path configuration and crossed paths are used to increase measuring accuracy, the error due to flow field distortions can not be ignored. This paper focuses on the numerical approach to estimate the accuracy of ultrasonic flowmeter under the disturbed flow condition. The flow field in the ultrasonic flowmeter can be simulated using FLUENT, and virtual acoustic paths are placed to investigate the flow error, which is the difference between the indicated flow and the real flow. The indicated flow can be integrated from the projected velocities on the acoustic paths, and the real flow can be calculated from the node velocities of the measuring section. To give a clear description, the flow error is divided to two parts: the axial error arising from the numerical integration of the axial velocities and the transverse error due to transverse flow effects. As an example, based on the simulated flow field in the penstock of the 3-Gorge hydropower station, the flow error is estimated, and the influence of the number of acoustic paths is analyzed, which may provide a suggestion for ultrasonic flowmeter design under the similar flow condition.

Key words: 3-Gorge power station, ultrasonic flowmeter, accuracy estimation, CFD

1. Introduction

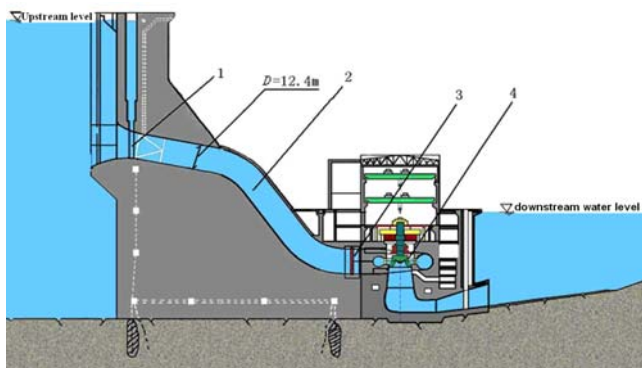
The global shortage of energy resources and water resources has brought about a rapid development of large hydraulic engineering and water transferring projects in China. For those projects, discharge measurement is of great importance. However, large diameters of the conduits cause the inapplicability of regular flowmeters. The multi-path ultrasonic flowmeters developed and utilized in recent years have well solved the technical problems ^[1] in flow measurement of large diameter conduits. The 3-George power station is one of the largest hydraulic projects, and in parts of the turbine units of the 3-George power station multi-path ultrasonic flowmeters have been installed to measure the generating flow ^[2]. As the flowmeters in the 3-George have a diameter of 12.4m upon which the actual flow calibration is not available, the measurement accuracy can only be evaluated indirectly.

With the development of computer and numerical computing technologies, numerical simulation has gradually become one of the most important academic tools. The numerical method can be used to obtain the flow field under complex conduit conditions, and to simulate multi-path ultrasonic flowmeters in numerical flow field. With the velocity distribution on different paths obtained using the interpolation algorithm, the indicated flow-rate of the flowmeter is calculated. And by comparing it with the actual flow-rate of the flow field, the measurement accuracy of the ultrasonic flowmeter is analyzed.

2. Flow analysis in flowmeter conduit

The installation conditions of the ultrasonic flowmeter are very strict, that is, an upstream straight conduit with length of at least 10D and a downstream straight conduit with length of at least 3D should be reserved to ensure a simple and smooth flow inside the conduit [3]. Due to the limits to site installation, the ultrasonic flowmeters have to be installed at the end of penstocks of the 3-George Station as is shown in Fig.1. The ultrasonic flowmeter is closely adjacent to the conduit bent upstream, and the turbine unit downstream, with hardly any straight conduit, which makes the flow field conditions in the flowmeter complex. So, the accuracy of the flowmeter will be affected by the complex flow field to some extent, although the configuration of two planes with nine chordal paths each has been adopted [4].

A numerical simulation for the internal flow of the penstocks in 3-George was performed using FLUENT. The computed fields along the water flow direction included reservoir, penstocks, turbine shells, vanes and draft tubes, as the computing grid is shown in Fig.2. Hexahedron grid is used and near-wall mesh is refined. The refinement is very important to obtain accurate near-wall velocities for the average velocity integration on the acoustic paths. As the main concern of the calculation is upon the flow field in the flowmeter, reservoir upstream is modeled to a pressure tank, whose front surface is the velocity inlet of the flow. The conduit wall is assumed to be hydraulically smooth under the no-slip boundary conditions. Reynolds stress model (RSM) is adopted for the turbulence, and QUICK scheme is used for the convection terms discretization, and a convergence solution is obtained.



1-sluice-gate 2-penstock 3-flowmeter 4-turbine
Fig.1. Sketch of flow passage of the power station

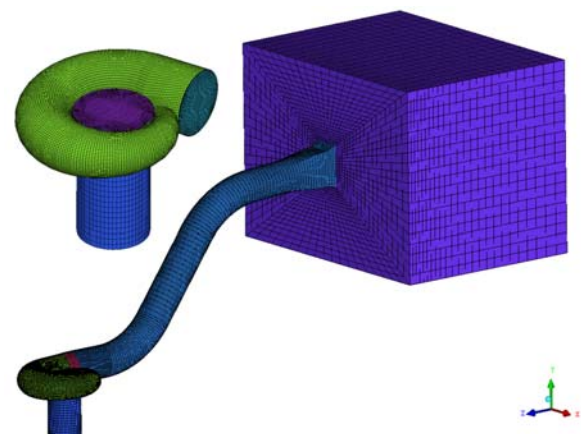


Fig.2 Computing grid

Flow field in the flowmeter is the basis for analyzing flowmeter accuracy. After the numerical flow field is obtained, a self-provided “scheme” language of FLUENT is used to extract the 3-D velocity onto the acoustic paths. The acoustic paths are horizontally arranged and the two planes with 9 paths each are crossed. The 3-D velocities corresponding to the center of each grid have been obtained from CFD data. In order to further analyze the flow errors of the flowmeter, the endpoint coordinates of the acoustic paths are determined, and then the 3-D velocities on acoustic paths of the flowmeter are extracted via linear interpolation.

Fig.3 shows the 3-D velocities on acoustic paths of the plane A when the average velocity $\bar{v} = 5\text{m/s}$. The four subfigures show the velocity vector and the three components of the velocity vector respectively. The former three are sketched in the same scale, and the last one is sketched in a scale 5 times zoomed in as its value is too small. Significant transverse flow in the flowmeter is observed. Among the two transverse components, V_y is vertical to the acoustic paths with no contribution to acoustic path velocity, while V_z has a certain intersection angle with the acoustic paths with a not negligible contribution to acoustic path velocity.

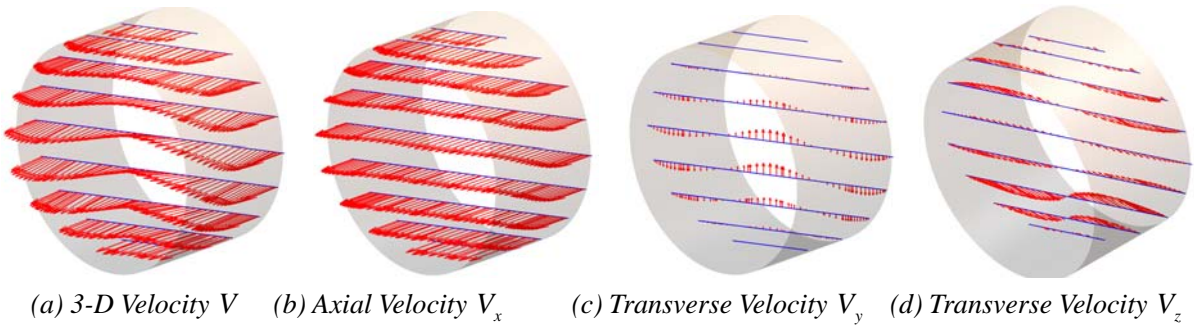


Fig.3 Velocity distribution of the acoustic paths

3. Calculation of acoustic path velocity

As difference exists among the transit time when the ultrasonic wave travels in the flow fluid, the values of ultrasonic transit time downstream and upstream, $t_{d,i}$ and $t_{u,i}$, are measured with a pair of transducers of the ultrasonic flowmeter, and then the acoustic path velocity can be obtained as follow,

$$\bar{v}_i = \frac{L_i}{2 \cos \phi_i} \left(\frac{1}{t_{u,i}} - \frac{1}{t_{d,i}} \right) \quad (1)$$

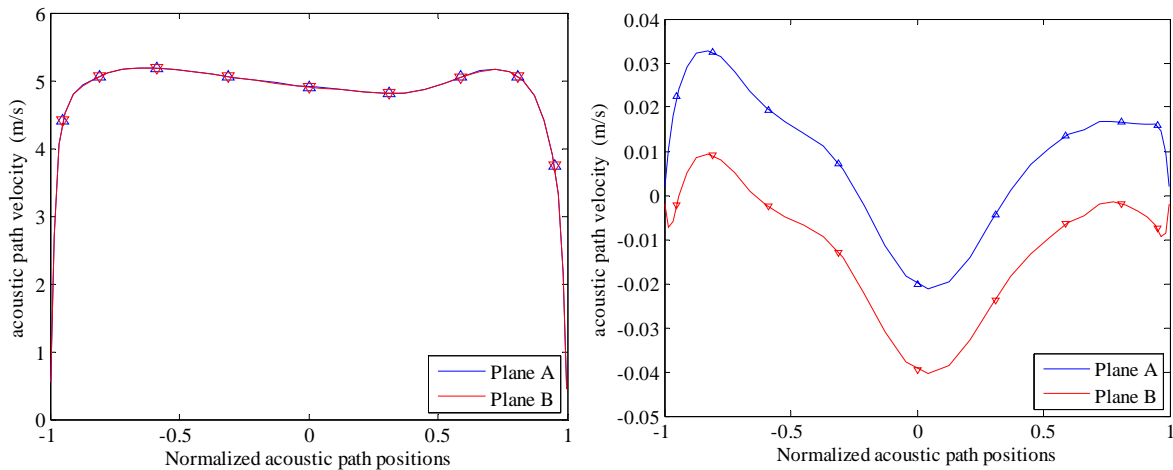
Where, L_i is the length of the acoustic path; ϕ_i is the acoustic path angle (an intersection angle between the acoustic path and the conduit axial line). It has been proved that the acoustic path velocity is far smaller than the acoustic velocity in water, and there is no curvature of the acoustic path, and thus the velocity expressed by Formula (1) can be regarded as the linear mean velocity on the acoustic path [5]. In addition, the measuring section can be divided into several parallel strips corresponding to the configuration of flowmeter, on each of which, the acoustic path velocity can represent the average velocity of the corresponding strip area. So the weighted average of the acoustic path velocities can be considered as the average velocity of the measuring section.

The flowmeter is expected to measure the axial flow velocity via acoustic path velocities, but transverse flow is also included in the acoustic path velocity when there is transverse flow. Acoustic path velocities are calculated based on the numerical flow field as showed in Fig.4. 3-D velocities on each node should be projected onto the acoustic path, and then converted to axial component as follows,

$$v_j = (v_j^x, v_j^y, v_j^z) \cdot \frac{(\Delta x, \Delta y, \Delta z)}{\Delta x} = v_j^x + \frac{v_j^y \Delta y + v_j^z \Delta z}{\Delta x} = v_j^x + v_j^{yz} \quad (2)$$

Where, the subscript j stands for the node on each acoustic path; $(\Delta x, \Delta y, \Delta z)$ is the direction of acoustic path. Acoustic path velocity can be integrated from each v_j . As the flowmeter is expected to measure the axial velocity v_j^x , the transverse velocity v_j^{yz} is a no-needed contribution of acoustic path velocity which will produce a transverse flow error.

Fig.4 shows the contributions of the axial and transverse flows on the acoustic path velocity when the average pipe velocity $\bar{v} = 5\text{m/s}$. The contribution of the axial flow to the acoustic path velocity is far greater than that of the transverse flow. The contributions of the axial flow to the acoustic path velocities of plane A and plane B are basically the same, while the contributions of the transverse flow to the acoustic path velocities of plane A and plane B are quite different. In addition, the positive A values and negative B values can be partially neutralized, which is an important reason why the disturbance of the transverse flow can be offset by the double-plane configuration of the flowmeter.



(a) Velocity contribution of the axial flow (b) Velocity contribution of the transverse flow
 Fig.4 Velocity contribution of the axial and transverse flow

The simulation results of acoustic path velocity (including the contribution of both the axial flow and the transverse flow) and the historic records of 3-George flowmeters in the same flow-rate condition are compared, as is shown in Fig.5, which indicates a perfect match with a common distribution pattern of acoustic path velocity: It suggests that the numerical result can reveal the actual flow field in the penstocks of 3-George station.

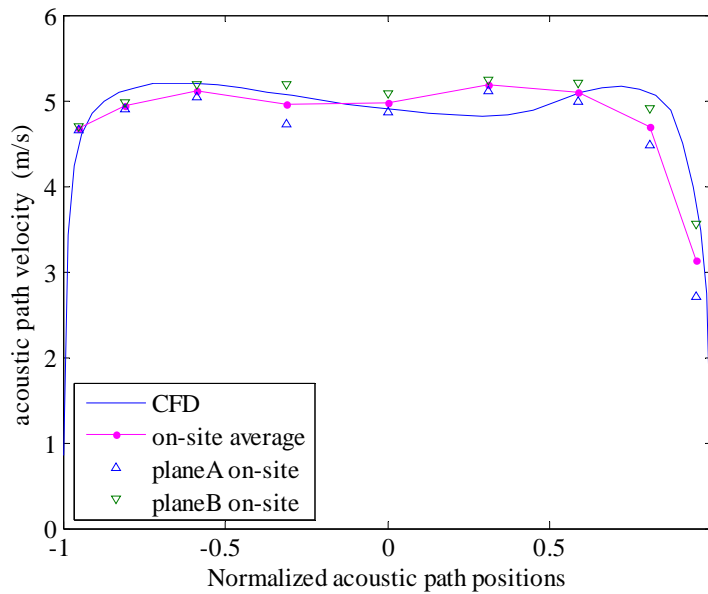


Fig.5 CFD velocity distribution vs. observed results

4. Flow error related to the complex flow field

With multiple acoustic paths applied in parallel on the measuring section by the ultrasonic flowmeter, the flow-rate can be calculated using the weighted sum method as follows,

$$Q = R \cdot \sum_{i=1}^N \omega_i \cdot \bar{v}_i \cdot l_i = R \cdot \sum_{i=1}^N \omega_i \cdot \bar{v}_i \cdot L_i \sin \phi_i \quad (3)$$

Where, R is the conduit radius; ω_i is the weighting coefficient; N is the number of the acoustic paths. In Formula (2), the acoustic path velocity is the projected velocity in the direction of acoustic paths, which can be decomposed into two contributions, axial and transverse velocities, so acoustic path velocity $\bar{v}_i = \bar{v}_i^x + \bar{v}_i^{yz}$. The flow-rate can be correspondingly decomposed into two

contributions, $Q_N = Q_N^x + Q_N^{yz}$. In addition, the 3-George flowmeter has two acoustic planes, and the flow indication is the average flow-rate of the two planes, $Q_9 = (Q_{A,9} + Q_{B,9})/2$.

Based on the numerical flow field, the actual flow-rate Q_s should be calculated from velocities of each node on the measuring section. The flow error (difference between the indication flow and actual flow) of the acoustic plane A can be decomposed into axial error and transverse error as follows,

$$Q_{A,9} - Q_s = (Q_{A,9}^x - Q_s) + Q_{A,9}^{yz} \quad (4)$$

Where, $(Q_{A,9}^x - Q_s)$ is caused by the uneven distribution of the flow field along the axial direction of the conduit; the transverse error $Q_{A,9}^{yz}$ is the disturbance of the transverse flow to the flow-rate. Both of them are physically clarified. For the convenience of statistics and analysis, the flow error is shown as relative values in percentage as is shown in Table 1. It can be seen that the axial error of the flowmeter is no more than 0.3% and the values of the two acoustic planes are almost the same, while the transverse errors of the two acoustic planes are respectively 0.1% and -0.3%, inversely marked and partly neutralized. Therefore, the transverse flow has bigger effects on the measurement accuracy of the flowmeter with single-plane configuration, while the average of the double acoustic planes can reduce the influence of the transverse flow, which quantitatively illustrates that it is better to apply the flowmeter on double-plane under the conditions of complex flow fields.

Table 1. Flow-rate errors at different average velocity

Mean velocity (m/s)	Plane A		Plane B		Average of plane A and B		
	Axial Error	Transverse Error	Axial Error	Transverse Error	Axial Error	Transverse Error	Total Error
1	0.33%	0.10%	0.25%	-0.29%	0.29%	-0.10%	0.19%
3	0.32%	0.08%	0.24%	-0.30%	0.28%	-0.11%	0.17%
5	0.34%	0.10%	0.25%	-0.31%	0.30%	-0.11%	0.19%

Different configurations of the acoustic paths are used in multi-path ultrasonic flowmeter, including different numbers of acoustic paths, different acoustic path angles and different rotation angles (the angle of the acoustic paths rotating around the conduit axis with zero on horizontal layout). In order to compare the effect of different acoustic path configuration, the factors such as rotation angles, acoustic path angles and acoustic path numbers are changed to make a statistical analysis on flow errors of flowmeter based on the flowmeter conduit flow fields with an average velocity of 5m/s, as is shown in Table 2.

It is found by comparing the influences of the rotation angles that there is no difference for double-plane flowmeter. Through the comparison of the influence of the acoustic path angles, axial errors are not directly related to the path angles, while the transverse errors increase with the path angles. This is favorable to the reduction of the theoretical errors of the flowmeter, but the measurement of axial velocity will be influenced if the acoustic path angle is too large, so a proper path angle should be chosen. Axial errors are greatly influenced by the acoustic path number, while the transverse error is not directly related to the acoustic path number. In fact, the transverse error is only related to the flowmeter conduit flow field. If the acoustic paths are located in transverse flow and the direction of transverse flows on the whole acoustic path line is consistent, there would be a large number of acoustic paths with rather great influence caused by the transverse flow.

Table 2. Effect of acoustic path configuration on flow-rate error

Case		Plane A		Plane B		Average of plane A and B		
		Axial Error	Transverse Error	Axial Error	Transverse Error	Axial Error	Transverse Error	Total Error
Rotation angle	-45	0.43%	0.51%	0.15%	-0.71%	0.29%	-0.10%	0.19%
	0	0.34%	0.10%	0.25%	-0.31%	0.29%	-0.11%	0.19%
	45	0.21%	-0.43%	0.37%	0.21%	0.29%	-0.11%	0.18%
	90	0.05%	-0.85%	0.38%	0.69%	0.22%	-0.08%	0.13%
Path angle	45	0.35%	-0.22%	0.11%	-0.41%	0.23%	-0.32%	-0.09%
	55	0.32%	0.00%	0.18%	-0.29%	0.25%	-0.15%	0.10%
	65	0.34%	0.10%	0.25%	-0.31%	0.29%	-0.11%	0.19%
	75	0.34%	0.25%	0.29%	-0.44%	0.31%	-0.10%	0.22%
Path number	2	1.89%	0.26%	1.80%	-0.16%	1.84%	0.05%	1.90%
	3	1.85%	0.01%	1.76%	-0.39%	1.80%	-0.19%	1.62%
	4	0.51%	0.16%	0.42%	-0.25%	0.46%	-0.05%	0.42%
	5	0.49%	0.07%	0.40%	-0.34%	0.44%	-0.14%	0.31%
	6	0.55%	0.10%	0.46%	-0.31%	0.50%	-0.11%	0.40%
	7	0.33%	0.10%	0.24%	-0.31%	0.28%	-0.11%	0.18%
	8	0.32%	0.09%	0.23%	-0.32%	0.27%	-0.12%	0.16%
	9	0.34%	0.10%	0.25%	-0.31%	0.29%	-0.11%	0.19%

5. Discussion on calculation of actual flow-rate

The indication flow-rate and actual flow-rate are needed for the analysis of flow errors caused by complex flow field. To calculate the former, the CFD flow field is interpolated onto the acoustic paths in the FLUENT software, and extracted to a ASCII file for the calculation of the acoustic path velocity, and then the indication flow-rates are calculated through weighted summation. To calculate the latter, node velocities of the measuring sections are extracted from the CFD flow field, and then with the triangular grids established, the average axial velocities at three fixed points of the triangle are taken as the average velocity on the triangular area to calculate the sum of the flow-rates on the whole section.

In fact, there are two more ways to calculate the actual flow-rate. Firstly, FLUENT can be directly used to calculate the flow-rate on a certain section by integrating, although the integral algorithm is unknown. Secondly, adequate acoustic paths can be applied according to the Gauss-Jacobi method in the numerical flow fields to calculate the indication flow-rate, which should be the same as the actual flow-rate if the truncation errors of values are not considered. Table 3 shows the result of the comparison using different algorithms to calculate the actual flow-rate when the average pipe velocity is 5m/s. Flow-rate calculations at the entrance of the computed field and on flowmeter section are conducted, and the difference between the two is very small, which indicates a numerical computing convergence. Flow-rate integration for the velocity of the axial flow on the section is carried out with Gauss-Jacobi method using 36 parallel acoustic paths (36 acoustic paths are enough; more paths make no difference) and different rotation angles, with no difference observed in the result. It is believed in this study that triangularization

quadrature is reasonable, because the same set of interpolation data is adopted to calculate the indication flow-rate. Meanwhile, there may be some system errors when FLUENT integration is directly used to determine the actual flow-rate.

Table 3. Difference between flow-rates determined by CFD data with different methods

Method	Triangularization quadrature	FLUENT integration		Gauss-Jacobi integration			
		Reservoir inlet	Flowmeter	36-path of simulated flowmeter			
Data position	Flowmeter			0	90	-45	45
Absolute Flow-rate	597.7666	603.8116	604.0195	599.0263	599.0621	599.0871	599.0873
Difference	0.00%	1.01%	1.05%	0.21%	0.22%	0.22%	0.22%

A numerical simulation on the complex flow conditions of 3-George penstock has been made by Rittmeyer ^{[6][7]}, which shows that a flow error of about -0.65% is generated with an 18-path flowmeter due to the flow field disturbance. Seen from their articles, the data is described as the total error, and the actual flow-rate is directly obtained by integration with the CFD software. In this study, the measurement error is obtained by extracting the CFD sectional flow field data and summing up after triangularization. Suppose the actual flow-rate referred to the flow field by Rittmeyer is about 1% greater than the result in this study, a total error of about 0.2% in this study will be very close to the result of about -0.6% obtained by Rittmeyer.

6. Conclusion

Numerical approach to estimate the accuracy of ultrasonic flowmeter under disturbed flow condition is established in this study. The flow error of the flowmeter caused by complex flow field conditions is analyzed by calculating the indication flow-rate and comparing with the directly-integrated actual flow-rate. The acquisition methods of actual flow-rates are discussed. It is considered better to extract sectional data and sum up after triangularization, with which the system error caused by numerical algorithms is reduced as much as possible.

FLUENT is used to calculate the flow field inside 3-George penstocks. The numerical result shows that the complex flow fields in the 3-George make the flowmeter indication increased by about 0.2%. As there are obvious transverse flows in the flowmeter, a quantificational analysis on the disturbance of transverse flows on the flow measurement is made. Double-plane configuration of the flowmeter can be used to neutralize transverse errors. Further discussions on the influence of different configuration on the flowmeter accuracy are also conducted. As to the special conformation of the penstock and double-plane configuration of the flowmeter in 3-George, rotation angles had no effect on flow error, while the path angle influenced the transverse error and the path number influenced the axial error.

The 3-George flowmeter had a large diameter, and thus the effect of the local disturbance of the sensor structure can be neglected. It should be noted that local disturbance of the smaller flowmeter greatly influenced its accuracy. It has been found that the protrusion effect of transducer with DN500 diameter caused a negative error more 1%. Further studies concerning this issue will be made.

Acknowledge

The authors gratefully acknowledge financial support from National Public Benefit (Quality Inspection) Research Foundation (Grant no. 2009424) and National High-tech R&D Program (Grant no. 2008AA042207).

References

- [1] Huo D Z. Large flow-rate measurement and multi-chords ultrasonic flowmeter (in Chinese). In Proceeding of the flow-rate measurement conference, 2006: 158-166.
- [2] Yi L, Li W X, Hou J J, et al. Discharge measurement system of three gorges right bank hydropower station (in Chinese). *Hydropower Automation and Dam Monitoring*, 2007, 31(6):43-45.
- [3] Tresch T, Gruber P, Staubli T: Comparison of integration methods for multi-path acoustic discharge measurements [A]. In proceeding of 6th International Conference on IGHEM, Portland, USA, 2006.
- [4] Grego G, Muciaccia F. Choice of the best position of 4 path acoustic systems in circular sections downstream curves or with inadequate straight pipes and disturbed speed profiles. In proceeding of 7th International Conference on IGHEM, Milan, Italy, 2008.
- [5] Moore P I, Johnson A N, Espina P I. Simulations of ultrasonic transit time in a fully developed turbulent flow using a ray-tracing method]. In Proceeding of the 22nd North Sea Flow Measurement Workshop, 2002.
- [6] Lüscher B, Staubli T, Tresch T, et al. Accuracy analysis of the acoustic discharge measurement using analytical, spatial velocity profiles. In proceeding of Hydro07, Granada, Spain, 2007.
- [7] Staubli T, Luescher B, Gruber P, et al. Optimization of acoustic discharge measurement using CFD. *International Journal on Hydropower & Dams*, 2008, 15(2): 109-112.